Thermophysical Properties of Amino Acid-Based Ionic Liquids

ARTICLE *in* JOURNAL OF CHEMICAL & ENGINEERING DATA · DECEMBER 2009

Impact Factor: 2.04 · DOI: 10.1021/je900660x

Thermophysical Properties of Amino Acid-Based Ionic Liquids

Ramesh L. Gardas,[†] Rile Ge,[†] Peter Goodrich,[†] Christopher Hardacre,*[,†] Azlan Hussain,[†,‡] and David W. Rooney[†]

The Quill Research Centre, School of Chemistry and Chemical Engineering, Queen's University Belfast, Belfast BT9 5AG, United Kingdom, and Petronas Research Sdn. Bhd., Tower 1, Petronas Twin Towers, Kuala Lumpur City Centre, 50088 Kuala Lumpur, Malaysia

Ionic liquids (ILs) having either cations or anions derived from naturally occurring amino acids have been synthesized and characterized as amino acid-based ionic liquids (AAILs). In this work, the experimental measurements of the temperature dependence of density, viscosity, heat capacity, and thermal conductivity of several AAILs, namely, tributylmethylammonium serinate ($[N_{4441}][Ser]$), tributylmethylammonium taurinate ($[N_{4441}][Tau]$), tributylmethylammonium lysinate ($[N_{4441}][Lys]$), tributylmethylammonium threonate ($[N_{4441}][Thr]$), tetrabutylphosphonium serinate ($[P_{4444}][Ser]$), tetrabutylphosphonium taurinate ($[P_{4444}][Tau]$), tetrabutylphosphonium lysinate ($[P_{4444}][Lys]$), tetrabutylphosphonium threonate ($[P_{4444}][Thr]$), tetrabutylphosphonium prolinate ($[P_{4444}][Pro]$), tetrabutylphosphonium valinate ($[P_{4444}][Val]$), and tetrabutylphosphonium cysteinate ($[P_{4444}][Cys]$), are presented. The influence of cations and anions on studied properties is discussed. On the basis of experimental data, the QSPR (quantitative structure−property relationship) correlations and group contribution methods for thermophysical properties of AAILs have been developed, which form the basis for the development of the computer-aided molecular design (CAMD) of AAILs. It has also been demonstrated that that the predictive data obtained by correlation methods are in good agreement with the experimental data. The correlations developed, herein, can thus be used to evaluate the studied thermophysical properties of AAILs for use in process design or in the CAMD of new AAILs.

Introduction

For more than a decade, ionic liquids (ILs) have attracted both industry and academia because of their physical and chemical properties. In particular, the large range of ion combinations that can induce specific IL behavior has resulted in them being termed as "designer solvents".[1−6] This concept relies on the fact that both chemical and physical properties may be changed at will; however, a focused design requires that some measure of predictability must be available, which can be difficult with so many combinations available.[1−6] Amino acid-based ionic liquids (AAILs) were first introduced by Fukumoto et al., wherein the AAIL was composed of imidazolium cations and amino acid anions,[7] and by Tao et al., who reported ILs compromising of cations derived from naturally occurring amino acids.[8] These materials have been shown to have a range of useful properties due to the fact that they contain two functional groups, a carboxylic acid and amino group, as well as the fact that a chiral center is present, which can be obtained relatively inexpensively using naturally derived amino acids.[7−12] Further characteristics of amino acid derived ILs include improved biodegradability[13] and biological activity.[14] Because of the fact that most of the reported AAILs are liquid at room temperature,[15] the synthetic methods for their formation are relatively atom-efficient,[16] and given that a wide variety of natural amino acids are available, a large increase in their usage has occurred.[7−12,15−24] For example, the AAIL properties have demonstrated applications in the areas of peptide synthesis and chiral catalysis[24] as well as use for bulk chemical processing such as in CO_2 capture.[18]

In this work, the experimental measurements of the temperature ($293.15 < T/K < 363.15$) dependence of density, viscosity, heat capacity, and thermal conductivity of several AAILs, namely, tributylmethylammonium serinate ($[N_{4441}][Ser]$), tributylmethylammonium taurinate ($[N_{4441}][Tau]$), tributylmethylammonium lysinate ($[N_{4441}][Lys]$), tributylmethylammonium threonate ($[N_{4441}][Thr]$), tetrabutylphosphonium serinate ($[P_{4444}][Ser]$), tetrabutylphosphonium taurinate ($[P_{4444}][Tau]$), tetrabutylphosphonium lysinate ($[P_{4444}][Lys]$), tetrabutylphosphonium threonate ($[P_{4444}][Thr]$), tetrabutylphosphonium prolinate ($[P_{4444}][Pro]$), tetrabutylphosphonium valinate ($[P_{4444}][Val]$), and tetrabutylphosphonium cysteinate ($[P_{4444}][Cys]$), are presented. The experimental densities were also correlated with the IL density estimation method proposed by Gardas and Coutinho.[25] The temperature dependence of the viscosity is represented by the Vogel−Fulcher−Tammann (VFT) empirical equation.[26] Experimental heat capacities of studied AAILs are predicted using the corresponding states method based on critical properties predicted using the modified Lydersen−Joback−Reid method employed by Ge et al.[27] and a second-order group additivity method proposed by Gardas and Coutinho.[28] The weak temperature dependence of the thermal conductivity is represented by a linear correlation.[26] Furthermore, the influence of cations and anions of AAILs on studied properties is discussed.

Experimental Section

Materials. AAILs, having $[N_{4441}]^+$ or $[P_{4444}]^+$ as a cation and an amino acid derivative as the anion, were prepared according to previously reported methods.[7,15,20] All amino acids, tributylmethylammonium hydroxide, $[N_{4441}][OH]$ (20 % by mass

* Corresponding author. Tel.: +44 28 9097 4592. Fax: +44 28 9097 4687. E-mail: c.hardacre@qub.ac.uk.
[†] Queen's University Belfast.
[‡] Petronas.

10.1021/je900660x
Published on Web 12/22/2009

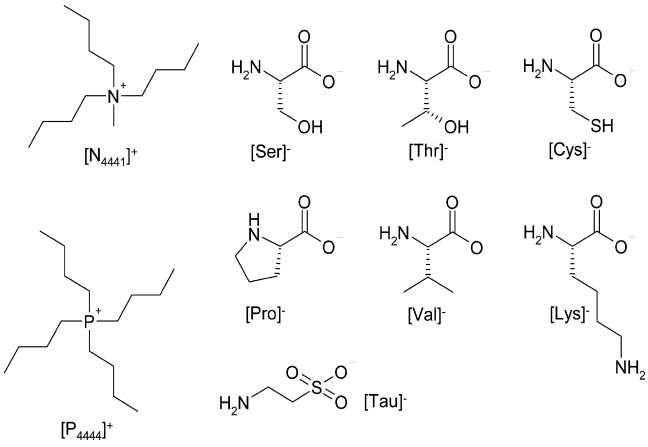

Figure 1. Structures of cations and anions of the AAILs studied. Cations: $[N_{4441}]^+$, tributylmethylammonium; $[P_{4444}]^+$, tetrabutylphosphonium. Anions: $[Ser]^-$, serinate; $[Thr]^-$, threonate; $[Lys]^-$, lysinate; $[Tau]^-$, taurinate; $[Pro]^-$, prolinate; $[Val]^-$, valinate; $[Cys]^-$, cysteinate.

Table 1. Molar Mass (M_{IL}), Water Content in Mass Fraction (w_w), Melting Point (T_m), Glass Transition Temperature (T_g), and Decomposition Temperature (T_d) of the AAILs Studied

	M_{IL}		T_m	T_g	T_d
IL	g·mol^{-1}	$w_w \cdot 10^3$	K	K	K
$[N_{4441}][Ser]$	304.47	0.041	ND[a]	222.56	439.74
$[N_{4441}][Tau]$	324.52	0.048	ND	218.92	461.74
$[N_{4441}][Lys]$	345.57	0.043	ND	213.76	426.05
$[N_{4441}][Thr]$	318.50	0.049	ND	221.21	437.03
				213.77	517.39
$[P_{4444}][Ser]$	363.53	0.053	ND	213.25[b]	516.15[b]
				211.70[c]	493[c]
$[P_{4444}][Tau]$	383.59	0.064	ND	215.01	649.16
				206.40	550.97
$[P_{4444}][Lys]$	404.63	0.051	ND	214.35[b]	550.15[b]
				208.01[c]	498[c]
$[P_{4444}][Thr]$	377.56	0.050	ND	212.43	496.19
$[P_{4444}][Pro]$	373.57	0.051	ND	207.28	572.04
$[P_{4444}][Val]$	375.59	0.045	298.92	207.59	553.81
$[P_{4444}][Cys]$	379.60	0.050	ND	243.47	463.77

[a] ND: not detected. [b] Ref 20. [c] Ref 18.

aqueous solution), and tetrabutylphosphonium hydroxide $[P_{4444}][OH]$ (40 % by mass aqueous solution) were purchased from Sigma Aldrich. To ensure the correct 1:1 stoichiometry (hydroxide/amino acid), the ammonium and phosphonium hydroxide solutions were titrated using a Metrohm 785 DNP potentiometric titrator. All AAILs studied were miscible with water; therefore, for the removal of excess free amino acid, the crude ILs were washed with mixed solvent (9:1 v/v) of acetonitrile and methanol. The AAILs were dried under vacuum (0.1 Pa) at 348 K for at least 48 h to reduce the water content and volatile compounds to negligible values prior to their use. The purity of each AAIL was checked by ^1H and ^{13}C NMR spectra which were recorded on Bruker Avance 300 MHz NMR spectrometer, using D_2O as the solvent. The structures of the cations and anions of AAILs studied are shown in Figure 1. The water content of the AAILs, shown in Table 1, was determined using a Mettler Toledo DL31 titrator with an uncertainty of 0.3 % using the Karl Fischer method. The analyte used for the coulometric Karl Fischer titration was Hydranal-Coulomat AG from Riedel-de Haën. All samples were dried and stored under dry nitrogen in a septum sealed flask. Approximately 0.1 g was used in the measurement.

Experimental Procedure. Melting points (T_m) and glass transition temperatures (T_g), with an uncertainty of 0.01 K, were determined using differential scanning calorimetry (DSC Q2000, TA Instruments) with constant heating of 10 K·min^{-1} and constant cooling of 5 K·min^{-1} within the predetermined temperature limit. A known amount of sample (5 to 10 mg) was placed in an alumina pan which was then hermetically sealed. The heating and cooling cycles were then repeated for a minimum of four cycles to ensure reproducibility.[29] Dynamic thermal decomposition temperatures (T_d) were measured under a N_2 atmosphere using thermogravimetric analysis (TGA, TA Instruments) at a constant heating rate of 10 K·min^{-1} to prevent any oxidation of the sample during the measurement. The decomposition temperature is defined as the intersection of the baseline weight (after the drying step) and the tangent line derived from the decomposition curve, as previously described.[29,30] Again the samples were analyzed using an alumina pan. All of the temperatures (T_m, T_g, and T_d) reported, herein, were determined using the Universal Analyzer software version 4.5. Comparing the decomposition temperatures (T_d) of the $[N_{4441}]^+$ and $[P_{4444}]^+$ based ILs with a common anion, T_d for $[P_{4444}]^+$ ILs are higher (59 to 187) K than that of $[N_{4441}]^+$ ILs, which shows that the thermal stability of tetrabutylphosphonium amino acid ILs is better than that of tributylmethylammonium amino acid ILs.

Experimental densities were measured using an Anton Paar DMA 4500 vibrating tube digital densitometer. This instrument was fully automated and, therefore, the resonant frequency was automatically determined. The temperature in the cell was regulated to ± 0.01 K with a solid state thermostat. The experimental setup and calibration procedure, using vacuum, air, nitrogen, triply distilled water, and aqueous solutions of NaCl (molalities of 1 mol·L^{-1} and 3 mol·L^{-1}), for the density measurements have been previously described.[31] The repeatability of the density measurements was 10^{-4} g·cm^{-3}, and the results have an uncertainty to 10^{-3} g·cm^{-3} using a sample size of 1 cm^3. The effect of the viscosity on the density measurement was analyzed to validate the density measurements. The density was found to vary by < 0.1 % and, therefore, was considered to be negligible.

Viscosities were measured using a Brookfield DV-II + PRO digital viscometer attached with a thermostat bath (Grant Instruments, model LTD6G) controlled to ± 0.01 K. To minimize the uncertainty caused by temperature equilibrium, all measurements were performed in triplicate or until constant reading obtained by taking each reading at 10 min intervals. The repeatability of the viscosity measurements was ± 0.2 % using a sample size of 2 cm^3, and a series of polydimethylsiloxane (PDMS) oils (Aldrich) covering viscosities from (1 to 100 000) mPa·s was used to calibrate the instrument.

A DSC Q2000 (TA Instruments) was used for the direct measurement of heat capacity using modulated DSC (MDSC) technology, with constant heating of 10 K·min^{-1} and constant cooling of 5 K·min^{-1}. Using MDSC technology, heat flow can be measured simultaneously with changes in heat capacity according to eq 1,

$$\frac{dH}{dt} = C_P \frac{dT}{dt} + f(t, T) \quad (1)$$

where dH/dt is the total heat flow (sum of all thermal transitions) comprising a heat capacity component, $C_p(dT/dt)$, associated with reversible heat flow for example glass and melting transitions, and a kinetic component, $f(t,T)$, associated with nonreversible heat flow, for example, curing, volatilization, and decomposition. At least three independent values of heat capacity were obtained at each temperature. The repeatability of these measurements was 3 % using a sample size of between

Table 2. Experimental Densities (ρ) of the Dried AAILs Studied as a Function of Temperature at Atmospheric Pressure

T/K	ρ/(g·cm^{-3})			
	$[N_{4441}][Ser]$	$[N_{4441}][Tau]$	$[N_{4441}][Lys]$	$[N_{4441}][Thr]$
293.15	1.019	1.054	0.983	1.003
298.15	1.016	1.051	0.980	1.000
303.15	1.013	1.048	0.977	0.996
313.15	1.006	1.042	0.971	0.990
323.15	1.000	1.036	0.965	0.984
333.15	0.994	1.030	0.959	0.978
343.15	0.988	1.024	0.953	0.972
353.15	0.982	1.018	0.947	0.966
363.15	0.976	1.012	0.941	0.960
	$[P_{4444}][Ser]$	$[P_{4444}][Tau]$	$[P_{4444}][Lys]$	$[P_{4444}][Thr]$
293.15	0.996	1.030	0.971	0.983
298.15	0.992	1.027	0.968	0.980
303.15	0.989	1.024	0.964	0.977
313.15	0.983	1.018	0.958	0.971
323.15	0.977	1.012	0.952	0.965
333.15	0.971	1.005	0.946	0.959
343.15	0.965	0.999	0.940	0.953
353.15	0.959	0.993	0.934	0.947
363.15	0.953	0.987	0.929	0.941
	$[P_{4444}][Pro]$	$[P_{4444}][Val]$	$[P_{4444}][Cys]$	
293.15	0.996		1.037	
298.15	0.993		1.034	
303.15	0.989		1.030	
313.15	0.983	0.932	1.024	
323.15	0.977	0.926	1.018	
333.15	0.971	0.920	1.012	
343.15	0.965	0.914	1.005	
353.15	0.959	0.908	0.999	
363.15	0.953	0.902	0.993	

(5 and 10) mg. The results have an uncertainty of 5 % which has been verified by the measurement of the heat capacity of pure water.

For the studied AAILs, the thermal conductivities as a function of temperature were measured using a KD2 Pro thermal properties analyzer (Labcell Ltd., U.K.). This consists of a thermal probe (1.3 mm diameter, 60 mm length) containing a heating element and a thermoresistor. The thermal probe was inserted vertically into a sealed glass vial, containing approximately 25 cm^3 of the AAIL. Before each measurement, the sample vial was fully immersed in a temperature-controlled water bath (Grant GD120) and allowed to equilibrate at the desired temperature. To ensure reproducibility of the measurements, at least four measurements were taken at each temperature, with the interval of at least 15 min between measurements. Further details concerning the experimental procedure and calibration, using water and a standard sample of glycerol of known thermal conductivity, of the equipment for the thermal conductivity measurements have been described previously.[32] The uncertainty in the thermal conductivity measurements was 0.005 W·m^{-1}·K^{-1}, while the temperature has an uncertainty of ± 1 K.

Results and Discussion

Density. Density measurements of pure AAILs were carried out at temperatures ranging from (293.15 to 363.15) K at 0.1 MPa. The experimental density data obtained are reported in Table 2 for all of the pure ILs studied. For the ILs having the tributylmethylammonium cation, $[N_{4441}]^+$, the density decreased as a function of the amino acid anion in the order $[Tau]^- > [Ser]^- > [Thr]^- > [Lys]^-$. A similar trend was found for the ILs having the tetrabutylphosphonium cation, $[P_{4444}]^+$, with the density decreasing with the amino acid anion in the order $[Cys]^- > [Tau]^- > [Pro]^- \geq [Ser]^- > [Thr]^- > [Lys]^- > [Val]^-$. In general, the density of the AAILs decreased with an increase in alkyl chain length of the amino acid anion, from serinate to lysinate to threonate, as expected. Comparing the densities of the $[N_{4441}]^+$ and $[P_{4444}]^+$ based ILs with a common anion shows that the ammonium systems are between (1.2 and 2.5) % higher than the analogous phosphonium systems. At 298.15 K, the experimental densities of $[P_{4444}][Ser]$ (0.992 g·cm^{-3}) and $[P_{4444}][Lys]$ (0.968 g·cm^{-3}) are in good agreement with those reported by Zhang et al., (0.991 and 0.973) g·cm^{-3}, respectively.[18] As expected, the densities of all studied AAILs were found to decrease with an increase in temperature. For the studied AAILs, up to a 4.3 % decrement in the density is observed by increasing the temperature from (293.15 to 363.15) K. The variation of the density with temperature for the ILs is illustrated in Figure 2. A quadratic equation was used to fit the variation with temperature at 0.1 MPa of the form:

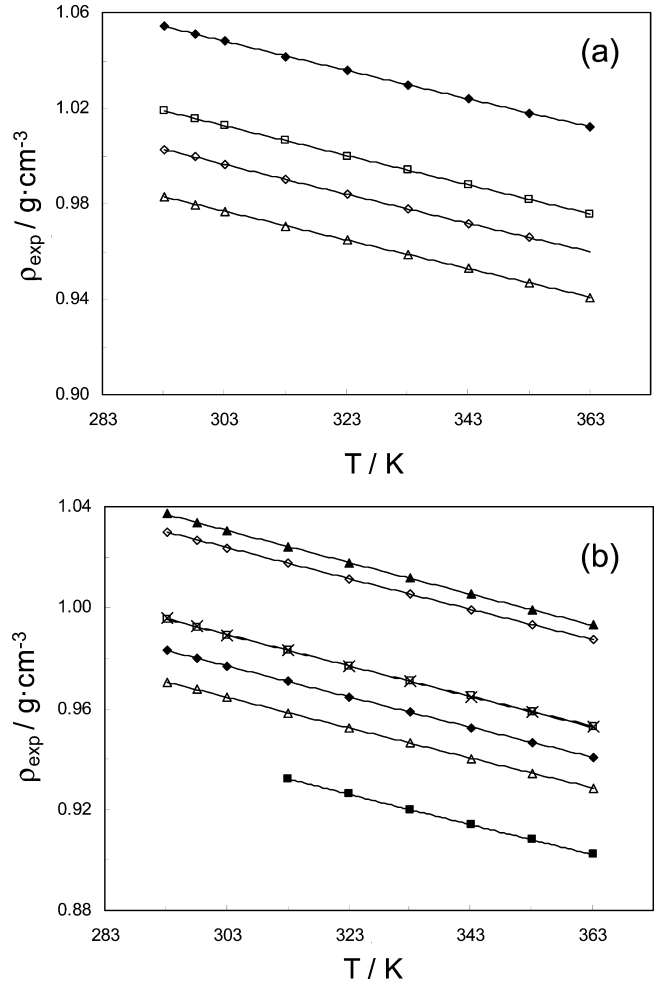

Figure 2. Experimental densities of the ILs studied as a function of the temperature at 0.1 MPa. (a) Effect of the amino acid-based anion on the densities of $[N_{4441}]^+$ based ILs: □, $[Ser]^-$; ◇, $[Thr]^-$; △, $[Lys]^-$; ◆, $[Tau]^-$. (b) Effect of the amino acid-based anion on the densities of $[P_{4444}]^+$ based ILs: □, $[Ser]^-$; ◇, $[Thr]^-$; △, $[Lys]^-$; ◆, $[Tau]^-$; ×, $[Pro]^-$; ■, $[Val]^-$; ▲, $[Cys]^-$. The solid lines correspond to the fit of the data by eq 2 using correlation parameters reported in Table 3.

$$\rho_{IL}(T) = \sum_{i=0}^{2} (a_i T^i) \quad (2)$$

with the parameters, a_i, given in Table 3 together with the absolute average deviation (AAD) and maximum absolute

Table 3. Correlation Parameters, a_i, from Equation 2, the AAD, and the MD for the Density of the AAILs Studied

IL	a_0 / g·cm^{-3}	$10^4\ a_1$ / g·cm^{-3}·K^{-1}	$10^7\ a_2$ / g·cm^{-3}·K^{-2}	AAD / %	MD / %
[N_{4441}][Ser]	1.22341	−7.6414	2.2605	0.008	0.018
[N_{4441}][Tau]	1.26622	−8.2318	3.4034	0.008	0.021
[N_{4441}][Lys]	1.17395	−6.9412	1.4370	0.005	0.008
[N_{4441}][Thr]	1.22837	−8.9771	4.3595	0.005	0.011
[P_{4444}][Ser]	1.20868	−8.2478	3.3249	0.002	0.003
[P_{4444}][Tau]	1.18700	−7.6910	2.5014	0.003	0.007
[P_{4444}][Lys]	1.17171	−7.5590	2.3782	0.004	0.008
[P_{4444}][Thr]	1.23475	−7.6968	2.4314	0.005	0.008
[P_{4444}][Pro]	1.20541	−7.9773	2.7983	0.007	0.020
[P_{4444}][Val]	1.15655	−8.1738	3.2143	0.002	0.002
[P_{4444}][Cys]	1.24873	−7.9920	2.6190	0.009	0.015

deviation (MD) for the density data of all of the studied ILs. The AAD is defined as:

$$\mathrm{AAD}\ (\%) = \frac{\sum_{i=1}^{N_p} |(\rho_{cal} - \rho_{exp})/\rho_{exp}|_i}{N_p} \qquad (3)$$

where cal and exp denote calculated and experimental properties, respectively, and N_p represents the number of experimental data points. An AAD of 0.005 % with the MD of 0.021 % was observed for the density correlation with temperature, using eq 2 with the parameters, a_i, given in Table 3, for the 96 density data points studied for the 11 AAILs.

Recently, Gardas and Coutinho proposed a predictive method[25] for the estimation of IL densities in a wide range of temperatures, (273.15 to 393.15) K, and pressures, (0.10 to 100) MPa, according to eq 4:

$$\rho_{IL}(T,P) = \frac{M}{NV(b + cT + dP)} \qquad (4)$$

where ρ is the density in g·cm^{-3}, M is molar mass in g·mol^{-1}, N is Avogadro's number, V is the molecular volume in m^3·10^{-30}, T is the temperature (K), and P is the pressure in MPa. The values of coefficients b, c, and d were estimated as $8.005 \cdot 10^{-1} \pm 2.3 \cdot 10^{-4}$, $6.652 \cdot 10^{-4} \pm 6.9 \cdot 10^{-7}$ K^{-1}, and $-5.919 \cdot 10^{-4} \pm 2.4 \cdot 10^{-6}$ MPa^{-1}, respectively, by fitting eq 4 to the previously published experimental pressure−volume−temperature (PVT) data of the ILs.[33,34]

The densities of the studied AAILs were estimated according to eq 4 with the molecular volumes V of ions and groups taken from previously reported values[25,35,36] where available. Since the molecular volumes of the studied amino acid anions were not available, these were estimated in this work by minimizing following objective function (OF):

$$\mathrm{OF} = \frac{\sum_{i=1}^{N_p} (\rho_{cal} - \rho_{exp})^2}{N_p} \qquad (5)$$

where ρ_{cal} is the calculated density using eq 4, ρ_{exp} is the experimental density, and N_p represents the number of data points. The molecular volumes of amino acid anions estimated in this work are presented in Table 4 together with the AAD and the MD observed. As shown in Figure 3a, the calculated density ρ_{cal} of the ILs studied displays a good agreement with the corresponding experimental density ρ_{exp}, where $\rho_{cal} = (1.0001 \pm 0.0002)\rho_{exp}$ ($R^2 = 0.9975$ at a 95 % level of confidence). For the density prediction from molecular volume, using eq 4, an AAD of 0.13 % with the MD of 0.50 % was observed for the 96 density data points studied for the 11 AAILs (Figure 3b).

Table 4. Density Correlation with Molecular Volume (V) Using Equation 4, the AAD, and the MD for the AAILs Studied

IL	$V \cdot 10^{-30}$/(m^3) cation[a]	$V \cdot 10^{-30}$/(m^3) anion[b]	data points	AAD / %	MD / %
[N_{4441}][Ser]	388	110	9	0.08	0.13
[N_{4441}][Tau]	388	123	9	0.27	0.50
[N_{4441}][Lys]	388	197	9	0.15	0.26
[N_{4441}][Thr]	388	141	9	0.09	0.18
[P_{4444}][Ser]	499	110	9	0.08	0.18
[P_{4444}][Tau]	499	123	9	0.28	0.46
[P_{4444}][Lys]	499	197	9	0.15	0.26
[P_{4444}][Thr]	499	141	9	0.07	0.18
[P_{4444}][Pro]	499	126	9	0.07	0.14
[P_{4444}][Val]	499	164	6	0.06	0.08
[P_{4444}][Cys]	499	111	9	0.08	0.13

[a] Ref 35. [b] Estimated in this work.

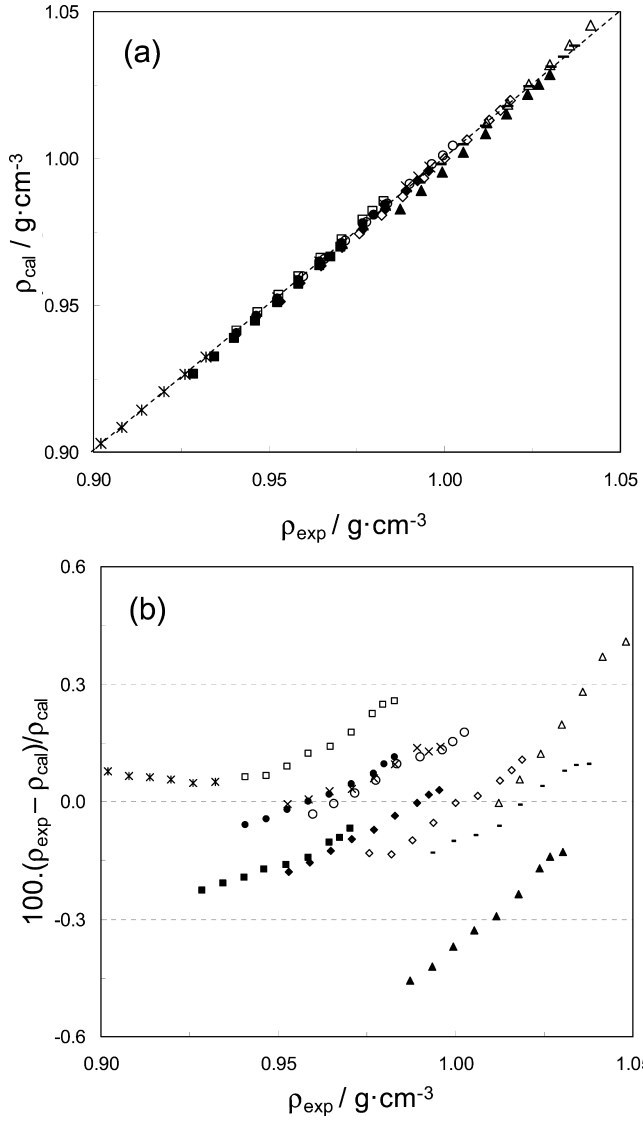

Figure 3. (a) Linear relationship between experimental and calculated density using eq 4 for the ILs studied. (b) The relative deviations between the calculated, using eq 4, and the experimental density data as a function of experimental density for the ILs studied. Symbols: ◇, [N_{4441}][Ser]; ○, [N_{4441}][Thr]; □, [N_{4441}][Lys]; △, [N_{4441}][Tau]; ◆, [P_{4444}][Ser]; ●, [P_{4444}][Thr]; ■, [P_{4444}][Lys]; ▲, [P_{4444}][Tau]; ×, [P_{4444}][Pro]; ∗, [P_{4444}][Val]; −, [P_{4444}][Cys].

Table 5. Experimental Viscosities (η) of the Dried AAILs Studied as a Function of Temperature at Atmospheric Pressure

T/K	η/(mPa·s)			
	$[N_{4441}][Ser]$	$[N_{4441}][Tau]$	$[N_{4441}][Lys]$	$[N_{4441}][Thr]$
298.15	10214	6674	2593	8368
303.15	5845	3965	1679	4916
313.15	2160	1600	741.4	1845
323.15	890.7	716.0	368.6	791.3
333.15	410.3	357.5	200.2	377.6
343.15	207.9	193.4	112.9	200.6
353.15	111.8	108.2	68.3	110.9
363.15	64.3	66.8	43.9	66.2
	$[P_{4444}][Ser]$	$[P_{4444}][Tau]$	$[P_{4444}][Lys]$	$[P_{4444}][Thr]$
298.15	1143	1019	741.0	739.0
303.15	778.4	712.6	519.8	519.8
313.15	395.4	345.5	268.7	260.1
323.15	209.4	186.2	149.7	143.2
333.15	122.9	106.7	90.4	88.5
343.15	77.6	67.5	59.8	53.9
353.15	49.7	44.2	39.7	36.2
363.15	34.1	29.6	27.5	25.1
	$[P_{4444}][Pro]$	$[P_{4444}][Val]$	$[P_{4444}][Cys]$	
298.15	1695		2946	
303.15	1101		1866	
313.15	483.5	216.9	832.7	
323.15	241.3	120.0	397.4	
333.15	133.1	70.8	208.4	
343.15	78.2	44.8	118.3	
353.15	49.6	29.6	72.5	
363.15	32.2	20.3	46.6	

Viscosity. Viscosity measurements of the AAILs were carried out at temperatures ranging from (298.15 to 363.15) K at 0.1 MPa. The experimental viscosity data obtained are reported in Table 5 for the ILs studied. For the $[N_{4441}]^+$ based AAILs, the viscosity was found to decrease with the amino acid anion with the following order, $[Ser]^- > [Thr]^- > [Tau]^- > [Lys]^-$. In contrast, the $[P_{4444}]^+$ based AAILs showed a variation of viscosity with the order [Cys] > [Pro] > [Ser] > [Tau] > [Lys] ≥ [Thr] > [Val]. Considering the case of AAILs having same anion, the viscosities of ILs having the $[N_{4441}]^+$ cation are much higher than that of the $[P_{4444}]^+$ cation. The experimental viscosity, at 298.15 K, of $[P_{4444}][Lys]$ (741 mPa·s) is in good agreement with the values reported by Zhang et al.[18] and Kagimoto et al.,[20] (744.71 and 779) mPa·s, respectively. In addition, the viscosity of $[P_{4444}][Cys]$ at 298.15 K (2946 mPa·s) is also in close agreement with the value (3029 mPa·s) reported by Kagimoto et al.[20] However, the experimental viscosity, at 298.15 K, of $[P_{4444}][Thr]$ (739 mPa·s) is lower than the value (965 mPa·s) reported by Kagimoto et al.,[20] while for $[P_{4444}][Ser]$, at 298.15 K, the viscosity reported, herein, (1143 mPa·s) is higher than both that reported by Zhang et al. (734.20 mPa·s)[18] and Kagimoto et al. (902 mPa·s).[20] It is well-known that the viscosity of ILs is significantly altered by the presence of small amounts of impurities such as water and, therefore, it is likely that these differences reflect small changes in the purity of the samples prepared. Some variation may also be expected by changes in the experimental techniques adopted; however, this is not likely to result in the present case.

As expected, the viscosities of all studied AAILs showed a marked decrease with increasing temperature. The variation of the viscosity with temperature for the ILs studied is illustrated in Figure 4a,b. A viscosity-temperature correlation based on the VFT equation (eq 6) is proposed:

$$\ln \eta = A + \frac{B}{(T - T_0)} \tag{6}$$

where η is viscosity in Pa·s units, T is temperature (K), and A, B, and T_0 are adjustable parameters. The ratio of parameters B and T_0, B/T_0, is also known as the Angell strength parameter. Experimental viscosity data of AAILs was used to optimize the parameters A, B, and T_0 simultaneously by minimizing following objective function (OF):

$$\mathrm{OF} = \frac{\sum_{i=1}^{N_p} \left(A + \frac{B}{(T - T_0)} - \ln \eta_{exp} \right)^2}{N_p} \tag{7}$$

The parameters A, B, and T_0 of eq 6, are given in Table 6 together with the AAD and MD for the viscosity data of all studied ILs. The values of the parameter T_0 obtained (Table 6) for all studied AAILs are close to the value obtained by Gardas and Coutinho,[26] 165.06 K, for approximately 500 viscosity data

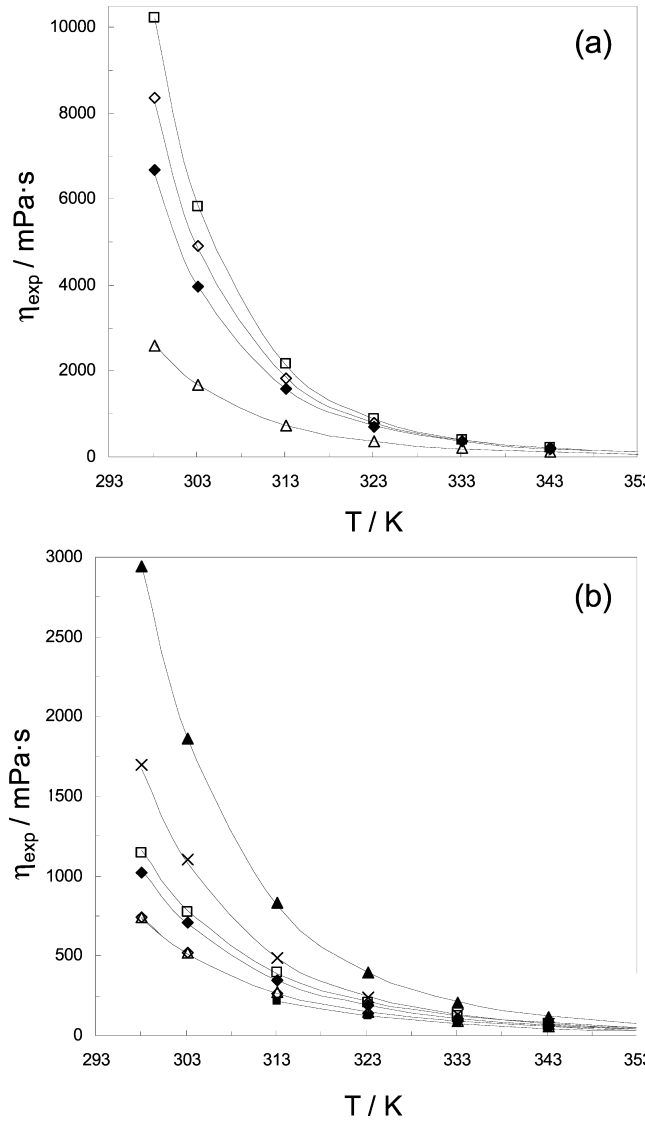

Figure 4. Experimental viscosities of the ILs studied as a function of the temperature at 0.1 MPa. (a) Effect of the amino acid-based anion on the viscosities of $[N_{4441}]^+$ based ILs: □, $[Ser]^-$; ◇, $[Thr]^-$; △, $[Lys]^-$; ◆, $[Tau]^-$. (b) Effect of the amino acid-based anion on the viscosities of $[P_{4444}]^+$ based ILs: □, $[Ser]^-$; ◇, $[Thr]^-$; △, $[Lys]^-$; ◆, $[Tau]^-$; ×, $[Pro]^-$; ■, $[Val]^-$; ▲, $[Cys]^-$. The solid lines correspond to the fit of the data by eq 6 using adjustable parameters reported in Table 6.

Table 6. Correlation Parameters A, B, and T_0 of Equation 6, Angell Parameter Strength (B/T_0), the AAD, and the MD for the Viscosity of the AAILs Studied

IL	A	B/K	T_0/K	B/T_0	AAD/%	MD/%
$[N_{4441}][Ser]$	−13.246	2096.69	163.51	12.82	0.30	0.45
$[N_{4441}][Tau]$	−12.108	1858.75	165.32	11.24	0.68	1.21
$[N_{4441}][Lys]$	−11.499	1664.53	164.62	10.11	0.85	1.38
$[N_{4441}][Thr]$	−12.409	1888.12	168.20	11.23	0.77	1.10
$[P_{4444}][Ser]$	−10.653	1448.23	164.05	8.83	0.90	1.26
$[P_{4444}][Tau]$	−10.769	1432.64	165.56	8.65	0.96	1.75
$[P_{4444}][Lys]$	−10.308	1332.89	164.86	8.09	1.03	1.56
$[P_{4444}][Thr]$	−10.590	1364.30	165.69	8.23	1.20	1.84
$[P_{4444}][Pro]$	−11.523	1589.69	166.08	9.57	1.52	2.06
$[P_{4444}][Val]$	−10.899	1388.23	164.96	8.42	0.29	0.29
$[P_{4444}][Cys]$	−11.749	1738.07	162.68	10.68	0.80	1.61

Table 7. Group Contribution Parameters A_i and B_i for Equation 8 for the Ammonium- and Phosphonium-Based ILs Studied

for ammonium-based ILs			for phosphonium-based ILs		
species	A_i	B_i/(K)	species	A_i	B_i/(K)
		Cations			
$[N_{1111}]^+$	−10.543	1320.81	$[P_{1111}]^+$	−9.250	805.15
		Anions			
$[Ser]^-$	−1.896	366.16	$[Ser]^-$	−0.455	135.21
$[Tau]^-$	−0.909	176.32	$[Tau]^-$	−0.634	144.05
$[Lys]^-$	−0.249	−33.89	$[Lys]^-$	−0.145	33.31
$[Thr]^-$	−1.423	274.80	$[Thr]^-$	−0.441	73.64
			$[Pro]^-$	−1.433	314.05
			$[Val]^-$	−0.745	91.15
			$[Cys]^-$	−1.438	390.33
		Groups			
CH_2[a]	$-7.528\cdot10^{-2}$	40.92	CH_2[a]	$-7.528\cdot10^{-2}$	40.92

[a] Values taken from ref 26.

points of 25 imidazolium, pyridinium, and pyrrolidinium based ILs.

By taking the parameter T_0 as constant, 165.06 K, for all studied AAILs, parameters A and B can be obtained by a group contribution method according to:

$$A = \sum_{i=1}^{k} n_i A_i \qquad B = \sum_{i=1}^{k} n_i B_i \tag{8}$$

where n_i is the number of groups of type i and k is the total number of different groups in the molecule; the parameters A_i and B_i are estimated according to the previously reported methods.[26] These parameters are presented individually for the ammonium- and phosphonium-based AAILs studied, herein, in Table 7.

As shown in Figure 5a, good agreement is observed between the calculated and the experimental viscosity data using the VFT equation (eq 5) with $T_0 = 165.06$ K and group contribution parameters A_i and B_i (Table 7) for the AAILs studied. The results indicate that the viscosity of studied AAILs decreases markedly with temperature increase, for example, on increasing the temperature by 5 K from (298.15 to 303.15) K a decrease in viscosity between (55 and 70) % was observed. This may be compared with a decrease in viscosity of (5 and 10) % for dodecane and water over the same temperature range.[37] The calculated viscosity (η_{cal}) of the AAILs studied displays a good agreement with the corresponding experimental viscosity (η_{exp}), where $\ln \eta_{cal} = (0.9647 \pm 0.0043)\ln \eta_{exp}$ ($R^2 = 0.9907$ at a 95 % level of confidence). Relative deviations between the calculated and the experimental viscosity data as a function of experimental viscosity for studied AAILs are shown in Figure 5b. The parameters A and B calculated from group contribution

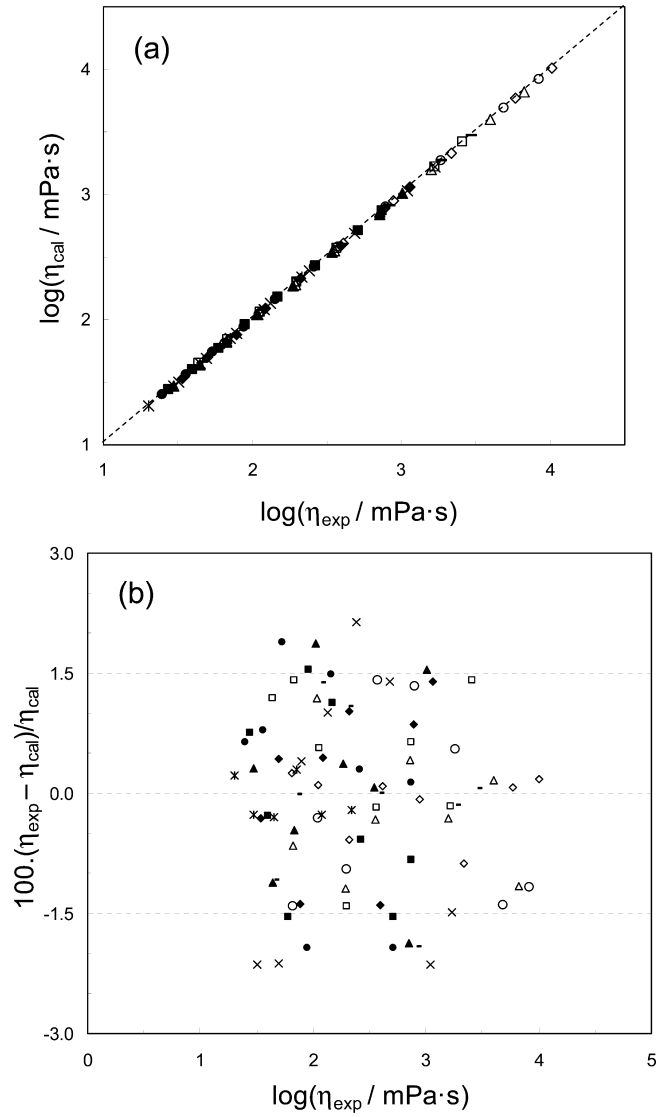

Figure 5. (a) Linear relationship between experimental and calculated viscosity using eqs 6 and 8 along with group contribution parameters A_i and B_i reported in Table 7 for the ILs studied. (b) The relative deviations between the calculated, using eqs 6 and 8, and the experimental viscosity data as a function of experimental viscosity for the ILs studied. Symbols: ◇, $[N_{4441}][Ser]$; ○, $[N_{4441}][Thr]$; □, $[N_{4441}][Lys]$; △, $[N_{4441}][Tau]$; ◆, $[P_{4444}][Ser]$; ●, $[P_{4444}][Thr]$; ■, $[P_{4444}][Lys]$; ▲, $[P_{4444}][Tau]$; ×, $[P_{4444}][Pro]$; ∗, $[P_{4444}][Val]$; —, $[P_{4444}][Cys]$.

Table 8. Parameters A and B Calculated from Group Contribution According to Equation 8, the AAD, and the MD for the Viscosity of the AAILs Studied

IL	A	B/K	data points	AAD/%	MD/%
$[N_{4441}][Ser]$	−13.117	2055.25	8	0.28	0.87
$[N_{4441}][Tau]$	−12.130	1865.41	8	0.68	1.19
$[N_{4441}][Lys]$	−11.470	1655.20	8	0.87	1.42
$[N_{4441}][Thr]$	−12.643	1963.89	8	1.07	1.41
$[P_{4444}][Ser]$	−10.608	1431.39	8	0.91	1.39
$[P_{4444}][Tau]$	−10.787	1440.24	8	0.95	1.87
$[P_{4444}][Lys]$	−10.298	1329.49	8	1.03	1.54
$[P_{4444}][Thr]$	−10.594	1369.82	8	1.14	1.93
$[P_{4444}][Pro]$	−11.586	1610.24	8	1.60	2.14
$[P_{4444}][Val]$	−10.899	1387.34	6	0.25	0.29
$[P_{4444}][Cys]$	−11.591	1686.52	8	0.71	1.92

according to eq 8 are given in Table 8 together with the AAD and the MD for the viscosity data of AAILs studied. For the 86 data points of 11 AAILs studied, the overall AAD was found to be 0.88 % with a maximum deviation of 2.14 %.

Table 9. Experimental Heat Capacities (C_p) of the Dried AAILs Studied as a Function of Temperature at Atmospheric Pressure

T/K	C_p/(J·mol^{-1}·K^{-1})			
	$[N_{4441}][Ser]$	$[N_{4441}][Tau]$	$[N_{4441}][Lys]$	$[N_{4441}][Thr]$
293.15	632	822	817	749
298.15	635	827	824	753
303.15	638	832	831	757
313.15	644	843	846	767
323.15	651	853	861	777
333.15	658	863	878	789
343.15	665	873	893	801
353.15	673	882	910	812
363.15	681	892	925	821
	$[P_{4444}][Ser]$	$[P_{4444}][Tau]$	$[P_{4444}][Lys]$	$[P_{4444}][Thr]$
293.15	742	988	987	952
298.15	749	995	997	961
303.15	755	1002	1004	971
313.15	766	1015	1021	992
323.15	777	1028	1040	1013
333.15	787	1043	1060	1033
343.15	798	1058	1078	1056
353.15	808	1074	1097	1076
363.15	815	1089	1112	1097
	$[P_{4444}][Pro]$	$[P_{4444}][Val]$	$[P_{4444}][Cys]$	
293.15	838	744	914	
298.15	844	747	920	
303.15	850	752	927	
313.15	864	761	943	
323.15	880	772	960	
333.15	895	781	977	
343.15	910	791	993	
353.15	926	801	1008	
363.15	939	811	1022	

Heat Capacity. Heat capacity was measured for 11 AAILs using DSC over the temperature range from (293 to 363) K. The experimental data obtained are reported in Table 9 and in Figure 6a,b. The heat capacities of the studied AAILs (in the range from (635 to 997) J·mol^{-1}·K^{-1} at 298.15 K) are much higher compared with traditional organic solvents. For example, at 298.15 K, the heat capacities of ethanol, toluene, and dodecane are (112, 158, and 376) J·mol^{-1}·K^{-1}, respectively.[37] For all AAILs studied, the relationship between heat capacity and temperature was found to be approximately linear, with an (8 to 14) % increase observed over the studied temperature range. Comparing the heat capacities of the AAILs with a common cation ($[N_{4441}]^+$ or $[P_{4444}]^+$), the heat capacity was found to decrease with the amino acid anion in the following order, $[Tau]^- \geq [Lys]^- > [Thr]^- > [Ser]^-$, and comparing the heat capacities of studied AAILs having a common anion shows that the phosphonium ILs ($[P_{4444}]^+$) are between (10 and 25) % higher than the analogous ammonium ($[N_{4441}]^+$) systems.

Ge et al.[27] used the modified Lydersen−Joback−Reid group contribution model to predict the IL heat capacities as a function of the temperature and also optimized new group parameters for the groups which are commonly found in ILs, such as P, B, and $-SO_2-$ groups. In the present study, the method employed by Ge et al.[27] was used to predict the heat capacity of the studied AAILs. The group parameters required for the calculations of ideal gas heat capacities, boiling points, and critical properties of studied AAILs are taken from literature,[27,38,39] except for the group parameters of ideal gas heat capacities for N and P atoms bonded to four other groups ($\rangle N\langle$ and $\rangle P\langle$, respectively), $-SO_2$ and $-SH$ groups which were optimized (by minimizing the deviation between experimental and predicted heat capacity data) in this work and presented in Table 10. The normal boiling point (T_b), critical temperature (T_c), critical pressure (P_c), critical volume (V_c), the acentric factor (ω), and group parameters for ideal gas heat capacities (A_{Cpk}, B_{Cpk}, C_{Cpk}, and D_{Cpk}) of studied AAILs were calculated according to the modified Lydersen−Joback−Reid group contribution model extended by Ge et al.[27] and presented in Table 11, together with the AAD observed between the calculated and the experimental heat capacity data. The relative deviations between these as a function of experimental heat capacity are shown in Figure 7. For the 11 AAILs studied, the AAD was in range of (0.2 to 13.4) % while the overall AAD for 99 data points was found to be 7.0 % with a maximum deviation of 14.2 %.

The heat capacities were also predicted using the second-order group additivity method, proposed by Gardas and Coutin

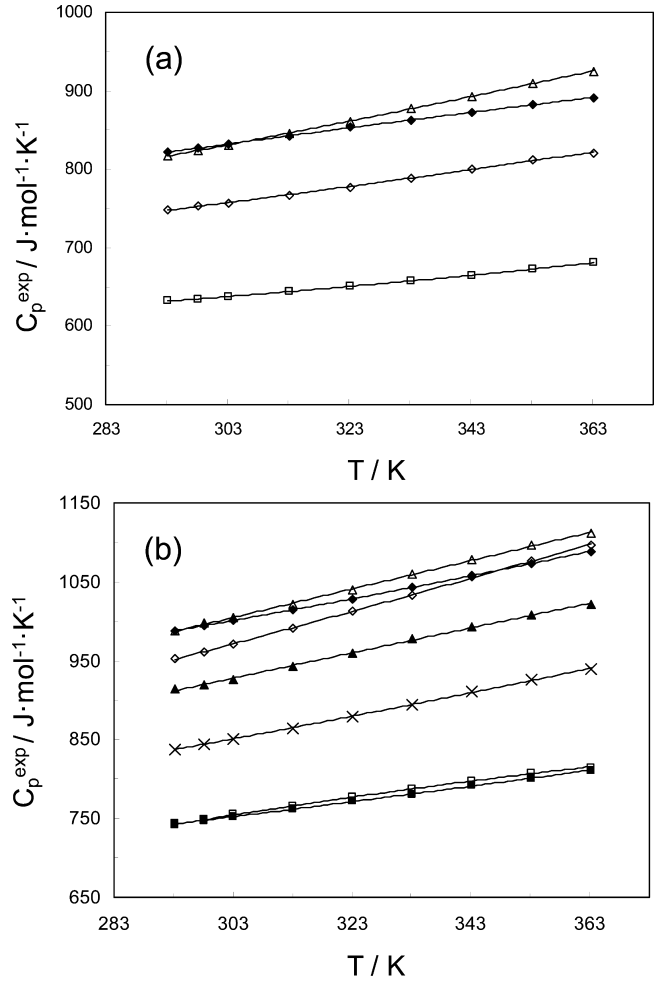

Figure 6. Experimental heat capacities of the ILs studied as a function of the temperature. (a) Effect of the amino acid-based anion on the densities of $[N_{4441}]^+$ based ILs: □, $[Ser]^-$; ◇, $[Thr]^-$; △, $[Lys]^-$; ◆, $[Tau]^-$. (b) Effect of the amino acid-based anion on the densities of $[P_{4444}]^+$ based ILs: □, $[Ser]^-$; ◇, $[Thr]^-$; △, $[Lys]^-$; ◆, $[Tau]^-$; ×, $[Pro]^-$; ■, $[Val]^-$; ▲, $[Cys]^-$.

Table 10. Group Parameters, Optimized in This Work, Required for an Ideal Gas Heat Capacity Calculation According to the Modified Lydersen−Joback−Reid Group Contribution Model

group	A_{Cpk} J·mol^{-1}·K^{-1}	10^3·B_{Cpk} J·mol^{-1}·K^{-2}	10^6·C_{Cpk} J·mol^{-1}·K^{-3}	10^8·D_{Cpk} J·mol^{-1}·K^{-4}
$\rangle N\langle$	−31.10	227	−1290	378
$\rangle P\langle$	−72.87	287	25.2	54.8
$-SO_2$	90.18	5.49	325	95.9
$-SH$	35.30	−75.8	939	4.14

Table 11. Critical Properties, Normal Boiling Temperature, Group Parameters for the Ideal Gas Heat Capacities of the AAILs Studied, Calculated According to the Modified Lydersen−Joback−Reid Group Contribution Model Extended by Ge et al.[27]

IL	T_b / K	T_C / K	P_C / $N \cdot m^{-2}$	V_C / $cm^3 \cdot mol^{-1}$	ω	A_{Cpk} / $J \cdot mol^{-1} \cdot K^{-1}$	B_{Cpk} / $J \cdot mol^{-1} \cdot K^{-2}$	$10^5 \cdot C_{Cpk}$ / $J \cdot mol^{-1} \cdot K^{-3}$	$10^6 \cdot D_{Cpk}$ / $J \cdot mol^{-1} \cdot K^{-4}$	AAD / %
$[N_{4441}][Ser]$	890.0	1079.7	14.8	1085.6	1.363	91.51	1.28	−106.8	3.37	11.21
$[N_{4441}][Tau]$	869.3	1090.8	19.1	1120.6	1.160	179.68	1.13	−61.4	4.29	2.67
$[N_{4441}][Lys]$	939.0	1137.8	12.7	1275.6	1.240	89.98	1.59	−124.4	3.40	0.88
$[N_{4441}][Thr]$	912.4	1105.6	14.2	1141.0	1.341	88.92	1.38	−112.6	3.38	5.02
$[P_{4444}][Ser]$	981.7	1188.0	12.8	1297.2	1.265	47.02	1.63	8.64	0.17	12.65
$[P_{4444}][Tau]$	961.1	1187.0	15.8	1332.2	1.193	135.19	1.48	54.1	1.09	5.00
$[P_{4444}][Lys]$	1030.7	1247.4	11.2	1487.3	1.143	45.49	1.94	−8.98	0.21	9.65
$[P_{4444}][Thr]$	1004.2	1215.2	12.3	1352.6	1.231	44.42	1.73	2.88	0.18	11.59
$[P_{4444}][Pro]$	932.0	1132.4	12.2	1340.0	1.172	9.89	1.73	14.6	0.10	4.26
$[P_{4444}][Val]$	934.9	1133.1	11.6	1389.0	1.155	38.22	1.79	0.48	0.18	13.44
$[P_{4444}][Cys]$	952.4	1159.9	14.0	1329.8	1.262	56.62	1.62	84.8	0.31	0.18

ho,[28] which employs a group contribution technique to estimate the D, E, and F parameters in eq 9:

$$C_P = R\left[D + E\left(\frac{T}{100}\right) + F\left(\frac{T}{100}\right)^2\right] \quad (9)$$

where R is the ideal gas constant ($R = 8.314\ J \cdot mol^{-1} \cdot K^{-1}$) and T is temperature (K). The group contributions to calculate D, E, and F parameters are obtained from:

$$D = \sum_{i=1}^{k} n_i d_i \qquad E = \sum_{i=1}^{k} n_i e_i \qquad F = \sum_{i=1}^{k} n_i f_i \quad (10)$$

where n_i is the number of groups of type I and k is the total number of different kinds of groups; the parameters d_i, e_i, and f_i estimated in this work for the studied AAILs are given in Table 12.

As shown in Figure 8a, good agreement is observed between the calculated and the experimental heat capacity data using the method proposed by Gardas and Coutinho,[28] eq 9, and group contribution parameters d_i, e_i, and f_i (Table 12). The calculated heat capacity (C_p^{cal}) of the AAILs studied displays a good agreement with the corresponding experimental heat capacity (C_p^{exp}), where $C_p^{cal} = (1.002 \pm 0.002) C_p^{exp}$ ($R^2 = 0.980$ at a 95 % level of confidence). Relative deviations between the calculated and the experimental heat capacity data as a function of experimental heat capacity are shown in Figure 8b. The parameters D, E, and F calculated from group contribution according to eq 10 are given in Table 13 together with the AAD and the MD. For the 99 data points of the 11 AAILs studied, the overall AAD was found to be 1.5 % with a maximum deviation of 4.2 %.

Table 12. Group Contributions for Parameters *D*, *E*, and *F* in Equation 10

species	d_i	e_i/(K)	f_i/(K^2)
Cations			
$[N_{1111}]^+$	6.994	11.887	−1.673
$[P_{1111}]^+$	17.854	8.200	−0.675
Anions			
$[Ser]^-$	29.849	−11.785	1.851
$[Tau]^-$	33.110	−1.177	0.849
$[Lys]^-$	25.123	−2.215	2.128
$[Thr]^-$	32.735	−7.320	2.253
$[Pro]^-$	6.232	3.656	0.190
$[Val]^-$	10.896	−1.337	0.036
$[Cys]^-$	24.206	−2.821	1.389
Groups			
CH_2[a]	−1.133	2.443	−0.259

[a] Values taken from ref 28.

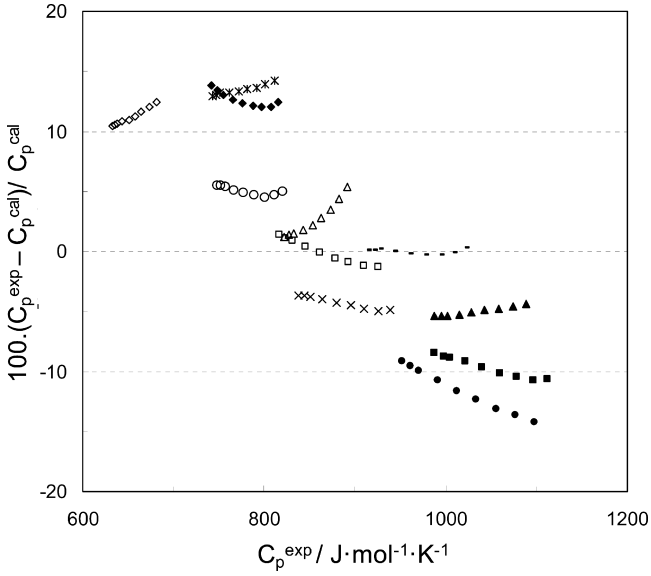

Figure 7. Relative deviations between calculated heat capacity using the Ge et al.[27] method and experimental heat capacity data as a function of experimental heat capacity for the ILs studied: ◇, $[N_{4441}][Ser]$; ○, $[N_{4441}][Thr]$; □, $[N_{4441}][Lys]$; △, $[N_{4441}][Tau]$; ◆, $[P_{4444}][Ser]$; ●, $[P_{4444}][Thr]$; ■, $[P_{4444}][Lys]$; ▲, $[P_{4444}][Tau]$; ×, $[P_{4444}][Pro]$; ∗, $[P_{4444}][Val]$; —, $[P_{4444}][Cys]$.

The deviations in the predicted heat capacity of the AAILs obtained by the Ge et al.[27] method are higher than that from the Gardas and Coutinho[28] method. This may be a consequence of the fact that the group parameters, used for the calculations of ideal gas heat capacities, boiling points, and critical properties in the method reported by Ge et al.,[27] were originally developed for molecular liquids, while in the case of the Gardas and Coutinho[28] method, the group parameters were developed specifically for ILs.

Thermal Conductivity. The thermal conductivity data for the 11 AAILs studied over the temperature range from (298 to 353) K are given in Table 14 and also presented in Figure 9a,b. All of the AAILs studied had similar thermal conductivities, within the range of (0.146 to 0.171) $W \cdot m^{-1} \cdot K^{-1}$. Thermal conductivities of all AAILs slightly decreased with the temperature increase. Comparing the thermal conductivities of the AAILs with a common cation ($[N_{4441}]^+$ or $[P_{4444}]^+$), it was found to decrease with the amino acid anion in the following order, $[Lys]^- > [Ser]^- > [Tau]^- > [Thr]^-$. Comparing the thermal conductivities of studied AAILs having a common anion shows that the ammonium ($[N_{4441}]^+$) are between (0.1 and 0.8) % higher than the analogous phosphonium ILs ($[P_{4444}]^+$) systems. Since thermal conductivity is weakly dependent on temperature, it could be fitted with a linear correlation of the form:

$$\lambda = \alpha T + \beta \qquad (11)$$

where T is temperature (K). The parameters, α and β of eq 11, are given in Table 15 together with the AAD and the MD. Using eq 11 along with the parameters shown in Table 15, for 75 data points of the 11 AAILs, the overall AAD was found to be 0.1 % with a maximum deviation of 0.3 %.

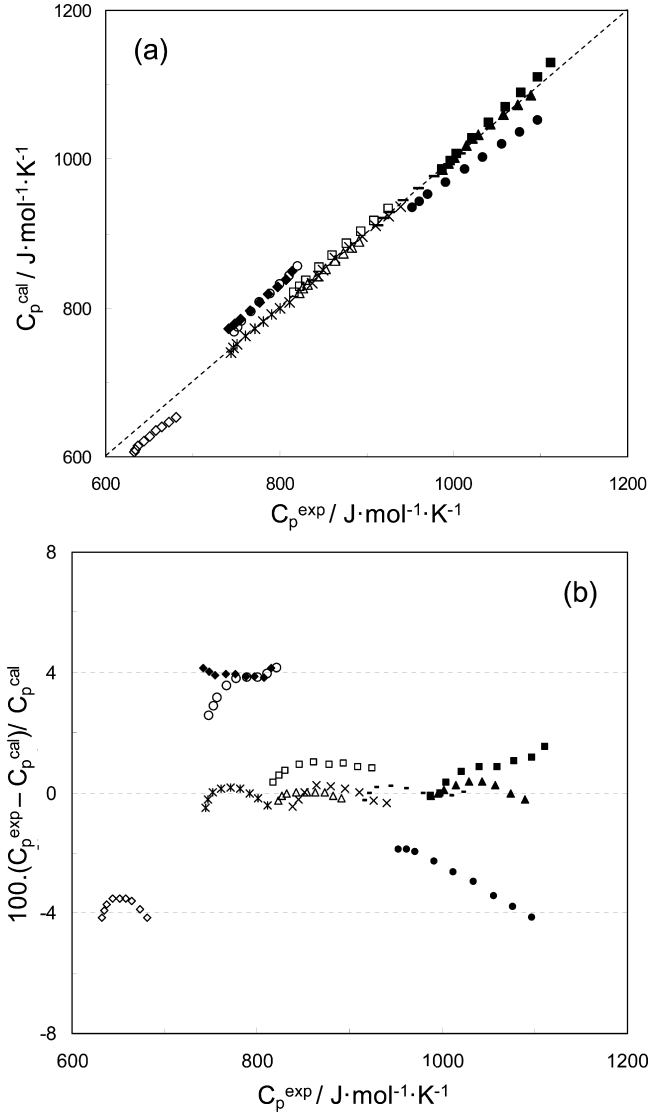

Figure 8. (a) Linear relationship between experimental and calculated heat capacity using eqs 9 and 10 along with group contribution parameters d_i, e_i, and f_i reported in Table 12 for the ILs studied. (b) The relative deviations between the calculated, using eqs 9 and 10, and the experimental heat capacity data as a function of experimental heat capacity for the ILs studied. Symbols: ◇, [N_{4441}][Ser]; ○, [N_{4441}][Thr]; □, [N_{4441}][Lys]; △, [N_{4441}][Tau]; ◆, [P_{4444}][Ser]; ●, [P_{4444}][Thr]; □, [P_{4444}][Lys]; ▲, [P_{4444}][Tau]; ×, [P_{4444}][Pro]; ∗, [P_{4444}][Val]; —, [P_{4444}][Cys].

Table 13. Parameters *D*, *E*, and *F* Calculated from Group Contribution According to Equation 10, the AAD, and the MD for the Heat Capacity of the AAILs Studied

IL	*D*	*E*/(K)	*F*/(K^2)	data points	AAD/%	MD/%
[N_{4441}][Ser]	26.65	22.09	−2.15	9	3.77	4.17
[N_{4441}][Tau]	29.91	32.70	−3.15	9	0.07	0.26
[N_{4441}][Lys]	21.92	31.66	−1.88	9	0.80	1.03
[N_{4441}][Thr]	29.53	26.55	−1.75	9	3.53	4.17
[P_{4444}][Ser]	34.11	25.73	−1.93	9	3.97	4.17
[P_{4444}][Tau]	37.37	36.34	−2.93	9	0.19	0.38
[P_{4444}][Lys]	29.38	35.30	−1.66	9	0.74	1.54
[P_{4444}][Thr]	36.99	30.20	−1.53	9	2.78	4.17
[P_{4444}][Pro]	10.49	41.17	−3.59	9	0.21	0.47
[P_{4444}][Val]	15.15	36.18	−3.75	9	0.19	0.48
[P_{4444}][Cys]	28.46	34.70	−2.39	9	0.12	0.27

Table 14. Experimental Thermal Conductivities (λ) of the Dried AAILs Studied as a Function of Temperature at Atmospheric Pressure

T/K	λ/(W·m^{-1}·K^{-1})			
	[N_{4441}][Ser]	[N_{4441}][Tau]	[N_{4441}][Lys]	[N_{4441}][Thr]
298.15	0.169	0.161	0.171	0.160
303.15	0.168	0.160	0.170	0.159
313.15	0.167	0.159	0.169	0.158
323.15	0.166	0.158	0.168	0.157
333.15	0.165	0.157	0.167	0.156
343.15	0.164	0.156	0.166	0.155
353.15	0.163	0.155	0.165	0.154
	[P_{4444}][Ser]	[P_{4444}][Tau]	[P_{4444}][Lys]	[P_{4444}][Thr]
298.15	0.161	0.160	0.163	0.156
303.15	0.160	0.160	0.163	0.155
313.15	0.159	0.159	0.162	0.154
323.15	0.158	0.158	0.161	0.153
333.15	0.157	0.157	0.160	0.152
343.15	0.156	0.156	0.159	0.152
353.15	0.155	0.155	0.158	0.151
	[P_{4444}][Pro]	[P_{4444}][Val]	[P_{4444}][Cys]	
298.15	0.154		0.152	
303.15	0.153		0.151	
313.15	0.152	0.157	0.150	
323.15	0.151	0.156	0.149	
333.15	0.150	0.155	0.148	
343.15	0.149	0.154	0.147	
353.15	0.148	0.153	0.146	

The parameters α and β can also be obtained from a group contribution approach as:

$$\alpha = \sum_{i=1}^{k} n_i \alpha_i \qquad \beta = \sum_{i=1}^{k} n_i \beta_i \qquad (12)$$

where n_i is the number of groups of type i and k is the total number of different groups in the IL; the parameters α_i, and β_i estimated for the studied AAILs are given in Table 16.

As shown in Figure 10a, good agreement is observed between the calculated and the experimental thermal conductivity data using the linear group contribution approach proposed by Gardas and Coutinho,[26] eq 11, and group contribution parameters α_i and β_i (Table 16) for the AAILs studied. The calculated thermal conductivity (λ_{cal}) of the AAILs displays good agreement with the corresponding experimental thermal conductivity (λ_{exp}), where $\lambda_{cal} = (0.9998 \pm 0.0010)\lambda_{exp}$ ($R^2 = 0.9435$ at a 95 % level of confidence). Relative deviations between the calculated and the experimental thermal conductivity data as a function of experimental thermal conductivity are shown in Figure 10b. The parameters α and β calculated from group contribution according to eq 12 are given in Table 17 together with the AAD and the MD. For the 75 data points the overall AAD was found to be 0.67 % with a maximum deviation of 1.85 %.

The QSPR (quantitative structure−property relationship) correlations and group contribution methods developed here are useful for predicting thermophysical properties necessary for the design of processes or products involving AAILs, and, furthermore, these models can provide the basis for the development of computer aided molecular design (CAMD) of AAILs. These equations allow rapid calculation, are facile to use, and can provide predictions of property values for AAILs other than those studied. For example, densities of six ILs based on the 1-ethyl-3-methylimidazolium cation with [Ser]$^-$, [Lys]$^-$, [Thr]$^-$, [Pro]$^-$, [Val]$^-$, and [Cys]$^-$ as the

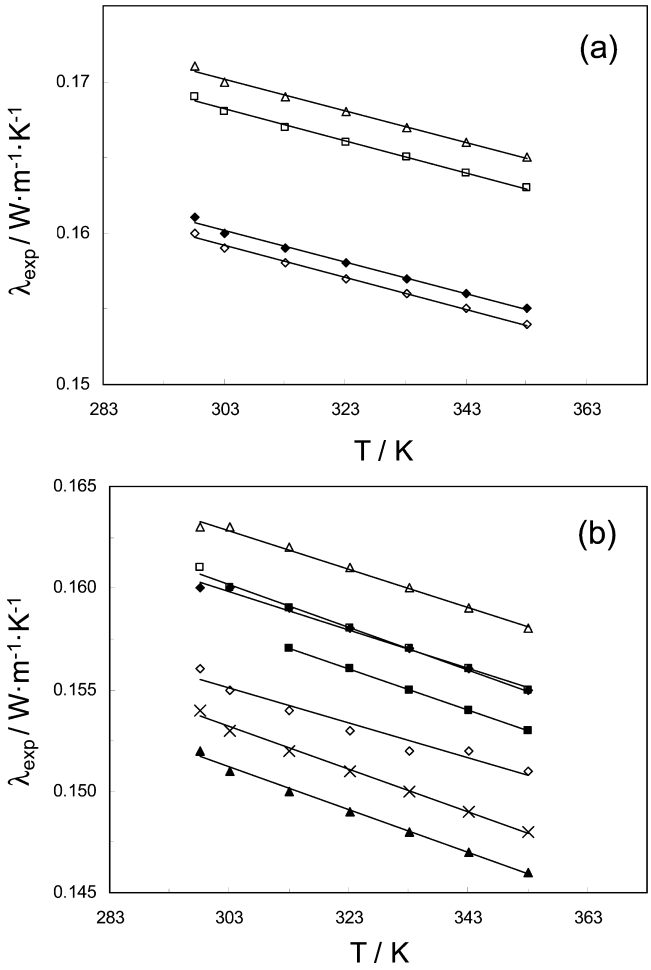

Figure 9. Experimental thermal conductivities of the ILs studied as a function of the temperature. (a) Effect of the amino acid-based anion on the thermal conductivities of $[N_{4441}]^+$ based ILs: □, $[Ser]^-$; ◇, $[Thr]^-$; △, $[Lys]^-$; ◆, $[Tau]^-$. (b) Effect of the amino acid-based anion on the thermal conductivities of $[P_{4444}]^+$ based ILs: □, $[Ser]^-$; ◇, $[Thr]^-$; △, $[Lys]^-$; ◆, $[Tau]^-$; ×, $[Pro]^-$; ■, $[Val]^-$; ▲, $[Cys]^-$. The solid lines correspond to the fit of the data by eq 11 using correlation parameters reported in Table 15.

Table 15. Correlation Parameters, α and *β*, from Equation 11, the AAD, and the MD for the Thermal Conductivities of the AAILs Studied

IL	$10^5 \cdot \alpha$ / W·m^{-1}·K^{-2}	β / W·m^{-1}·K^{-1}	AAD / %	MD / %
$[N_{4441}][Ser]$	−10.618	0.2004	0.08	0.14
$[N_{4441}][Tau]$	−10.785	0.1929	0.08	0.14
$[N_{4441}][Lys]$	−10.895	0.2033	0.09	0.13
$[N_{4441}][Thr]$	−10.632	0.1915	0.08	0.15
$[P_{4444}][Ser]$	−10.712	0.1927	0.08	0.14
$[P_{4444}][Tau]$	−9.060	0.1872	0.10	0.15
$[P_{4444}][Lys]$	−9.106	0.1904	0.09	0.14
$[P_{4444}][Thr]$	−8.863	0.1820	0.22	0.29
$[P_{4444}][Pro]$	−10.510	0.1851	0.09	0.15
$[P_{4444}][Val]$	−10.000	0.1883	0.01	0.01
$[P_{4444}][Cys]$	−10.089	0.1818	0.15	0.16

anion, at 298.15 K, were predicted using eq 4 with the anion molecular volumes *V* given in Table 4 [molecular volume for 1-ethyl-3-methylimidazolium cation is $(182 \cdot 10^{-30})$ m^3].[25] The predicted densities show good agreement with the density values obtained from molecular dynamics simulations by Sirjoosingh et al.[40] For the six data points, the AAD was found to be 0.9 % with a MD of 1.4 %. Similar correlations cannot be made, to date, for the thermophysical properties

Table 16. Group Contribution Parameters α_i and β_i for Equation 12 for Thermal Conductivities of the Ammonium- and Phosphonium-Based ILs Studied

species	$10^5 \cdot \alpha_i$ / W·m^{-1}·K^{-2}	β_i / W·m^{-1}·K^{-1}
	Cations	
$[N_{1111}]^+$	5.290	0.1625
$[P_{1111}]^{+a}$	3.230	0.1503
	Anions	
$[Ser]^-$	3.802	0.0301
$[Tau]^-$	4.149	0.0268
$[Lys]^-$	3.091	0.0301
$[Thr]^-$	1.629	0.0162
$[Pro]^-$	3.595	0.0208
$[Val]^-$	3.644	0.0259
$[Cys]^-$	3.705	0.0191
	Groups	
CH_2[a]	0.2586	0.0010

[a] Values taken from ref 26.

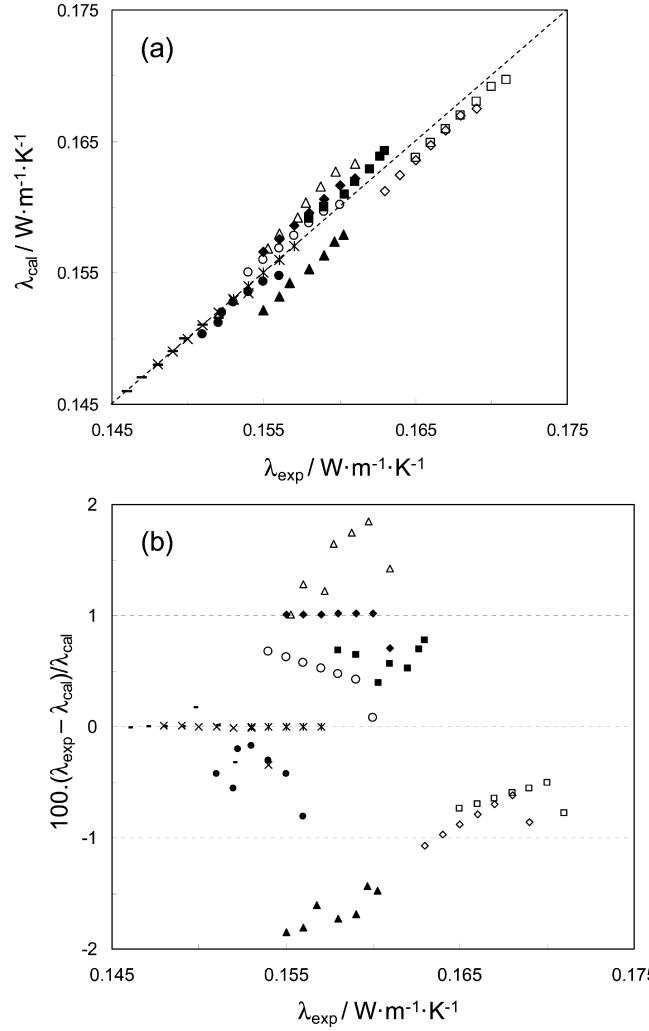

Figure 10. (a) Linear relationship between experimental and calculated thermal conductivity using eqs 11 and 12 along with group contribution parameters α_i and β_i reported in Table 16 for the ILs studied. (b) The relative deviations between the calculated, using eqs 11 and 12, and the experimental thermal conductivity data as a function of experimental thermal conductivity for the ILs studied. Symbols: ◇, $[N_{4441}][Ser]$; ○, $[N_{4441}][Thr]$; □, $[N_{4441}][Lys]$; △, $[N_{4441}][Tau]$; ◆, $[P_{4444}][Ser]$; ●, $[P_{4444}][Thr]$; ■, $[P_{4444}][Lys]$; ▲, $[P_{4444}][Tau]$; ×, $[P_{4444}][Pro]$; ∗, $[P_{4444}][Val]$; —, $[P_{4444}][Cys]$.

of other AAILs because of the lack of experimental data; however, as data becomes available, these group contribution methods will be developed further.

Table 17. Parameters α and β Calculated from Group Contribution According to Equation 12, the AAD, and the MD for the Thermal Conductivities of the AAILs Studied

	$10^5 \cdot \alpha$	β		AAD	MD
IL	$W \cdot m^{-1} \cdot K^{-2}$	$W \cdot m^{-1} \cdot K^{-1}$	data points	%	%
$[N_{4441}][Ser]$	11.419	0.2016	7	0.84	1.07
$[N_{4441}][Tau]$	11.766	0.1984	7	1.46	1.85
$[N_{4441}][Lys]$	10.708	0.2016	7	0.65	0.78
$[N_{4441}][Thr]$	9.247	0.1877	7	0.48	0.68
$[P_{4444}][Ser]$	10.135	0.1924	7	0.97	1.02
$[P_{4444}][Tau]$	10.482	0.1891	7	1.66	1.85
$[P_{4444}][Lys]$	9.424	0.1924	7	0.61	0.78
$[P_{4444}][Thr]$	7.962	0.1785	7	0.41	0.81
$[P_{4444}][Pro]$	9.928	0.1831	7	0.05	0.34
$[P_{4444}][Val]$	9.977	0.1882	5	0.01	0.01
$[P_{4444}][Cys]$	10.038	0.1814	7	0.07	0.32

Conclusions

Several ILs based on amino acid anions and either ammonium- or phosphonium-based cations were synthesized and their density, viscosity, heat capacity, and thermal conductivity measured as a function of temperature. The experimental data was used to develop QSPR correlations and group contribution models for the prediction of thermophysical properties of AAILs. Calculated thermophysical property values for the studied AAILs displayed a good agreement with the corresponding experimental data. The correlations developed here can be used to evaluate the thermophysical properties of AAILs for use in process design or in the CAMD of new AAILs.

Literature Cited

(1) Welton, T. Room-Temperature Ionic Liquids. Solvents for Synthesis and Catalysis. *Chem. Rev.* **1999**, *99*, 2071–2083.

(2) Pârvulescu, V. I.; Hardacre, C. Catalysis in Ionic Liquids. *Chem. Rev.* **2007**, *107*, 2615–2665.

(3) Heintz, A. Recent developments in thermodynamics and thermophysics of non-aqueous mixtures containing ionic liquids. A review. *J. Chem. Thermodyn.* **2005**, *37*, 525–535.

(4) Plechkova, N. V.; Seddon, K. R. Applications of ionic liquids in the chemical industry. *Chem. Soc. Rev.* **2008**, *37*, 123–150.

(5) Harper, J. B.; Kobrak, M. N. Understanding organic processes in ionic liquids: Achievements so far and challenges remaining. *Mini-Rev. Org. Chem.* **2006**, *3*, 253–269.

(6) Wasserscheid, P.; Welton, T. *Ionic Liquids in Synthesis*; Wiley-VCH: Weinheim, Germany, 2007.

(7) Fukumoto, K.; Yoshizawa, M.; Ohno, H. Room temperature ionic liquids from 20 natural amino acids. *J. Am. Chem. Soc.* **2005**, *127*, 2398–2399.

(8) Tao, G.; He, L.; Sun, N.; Kou, Y. New generation ionic liquids: cations derived from amino acids. *Chem. Commun.* **2005**, 3562–3564.

(9) Bao, W.; Wang, Z.; Li, Y. Synthesis of chiral ionic liquids from natural amino acids. *J. Org. Chem.* **2003**, *68*, 591–593.

(10) Guillen, F.; Brégeon, D.; Plaquevent, J. C. (S)-Histidine: the ideal precursor for a novel family of chiral aminoacid and peptidic ionic liquids. *Tetrahedron Lett.* **2006**, *47*, 1245–1248.

(11) Branco, L. C.; Gois, P. M. P.; Lourenço, N. M. T.; Kurteva, V. B.; Afonso, C. A. M. Simple transformation of crystalline chiral natural anions to liquid medium and their use to induce chirality. *Chem. Commun.* **2006**, 2371–2372.

(12) Luo, S.; Zu, D.; Yue, H.; Wang, L.; Yang, W.; Xu, Z. Synthesis and properties of novel chiral-amine-functionalized ionic liquids. *Tetrahedron: Asymmetry* **2006**, *17*, 2028–2033.

(13) Gathergood, N.; Garcia, M. T.; Scammells, P. J. Biodegradable ionic liquids: Part I. Concept, preliminary targets and evaluation. *Green Chem.* **2004**, *6*, 166–175.

(14) Docherty, K. M.; Kulpa, C. F., Jr. Toxicity and antimicrobial activity of imidazolium and pyridinium ionic liquids. *Green Chem.* **2005**, *7*, 185–189.

(15) Ohno, H.; Fukumoto, K. Amino Acid Ionic Liquids. *Acc. Chem. Res.* **2007**, *40*, 1122–1129.

(16) Li, W.; Qi, C.; Wu, X.; Rong, H.; Gong, L. Theoretical investigation of interactions between glycine cation based ionic liquids and water molecules. *J. Mol. Struct.: THEOCHEM* **2008**, *855*, 34–39.

(17) Ni, B.; Headley, A. D.; Li, G. Design and Synthesis of C-2 Substituted Chiral Imidazolium Ionic Liquids from Amino Acid Derivatives. *J. Org. Chem.* **2005**, *70*, 10600–10602.

(18) Zhang, J. M.; Zhang, S. J.; Dong, K.; Zhang, Y. Q.; Shen, Y. Q.; Lv, X. M. Supported Absorption of CO2 by Tetrabutylphosphonium Amino Acid Ionic Liquids. *Chem.—Eur. J.* **2006**, *12*, 4021–4026.

(19) Tao, G. H.; He, L.; Liu, W. S.; Lin, X.; Xu, L.; Xiong, W.; Wang, T.; Kou, Y. Preparation, characterization and application of amino acid-based green ionic liquids. *Green Chem.* **2006**, *8*, 639–646.

(20) Kagimoto, J.; Fukomoto, K.; Ohno, H. Effect of tetrabutylphosphonium cation on physio-chemical properties of amino acid ionic liquids. *Chem. Commun.* **2006**, 2254–2256.

(21) Yamada, T.; Lukac, P. J.; Yu, T.; Weiss, R. G. Reversible, Room-Temperature, Chiral Ionic Liquids. Amidinium Carbamates Derived from Amidines and Amino-Acid Esters with Carbon Dioxide. *Chem. Mater.* **2007**, *19*, 4761–4768.

(22) Tang, F.; Wu, K.; Nie, Z.; Ding, L.; Liu, Q. Quantification of Amino Acid Ionic Liquids using Liquid Chromatography-Mass Spectrometry. *J. Chromatogr., A* **2008**, *1208*, 175–181.

(23) Fang, D. W.; Guan, W.; Tong, J.; Wang, Z. W.; Yang, J. Z. Study on Physicochemical Properties of Ionic Liquids Based on Alanine [$C_n$mim][Ala] (n = 2,3,4,5,6). *J. Phys. Chem. B* **2008**, *112*, 7499–7505.

(24) Plaquevent, J. C.; Levillain, J.; Guillen, F.; Malhiac, C.; Gaumont, A.-C. Ionic Liquids: New Targets and Media for r-Amino Acid and Peptide Chemistry. *Chem. Rev.* **2008**, *108*, 5035–5060, plus references therein.

(25) Gardas, R. L.; Coutinho, J. A. P. Extension of the Ye and Shreeve group contribution method for density estimation of ionic liquids in a wide range of temperatures and pressures. *Fluid Phase Equilib.* **2008**, *263*, 26–32.

(26) Gardas, R. L.; Coutinho, J. A. P. Group Contribution Methods for the Prediction of Thermophysical and Transport Properties of Ionic Liquids. *AIChE J.* **2009**, *55*, 1274–1290.

(27) Ge, R.; Hardacre, C.; Jacquemin, J.; Nancarrow, P.; Rooney, D. W. Heat Capacities of Ionic Liquids as a Function of Temperature at 0.1 MPa. Measurement and Prediction. *J. Chem. Eng. Data* **2008**, *53*, 2148–2153.

(28) Gardas, R. L.; Coutinho, J. A. P. A Group Contribution Method for Heat Capacity Estimation of Ionic Liquids. *Ind. Eng. Chem. Res.* **2008**, *47*, 5751–5757.

(29) Croswaithe, J. M.; Muldoon, M. J.; Dixon, J. K.; Anderson, J. L.; Brennecke, J. F. Phase transition and decomposition temperature, heat capacities and viscosities of pyridinium ionic liquids. *J. Chem. Thermodyn.* **2005**, *37*, 559–568.

(30) Fredlake, C. P.; Crostwaite, J. M.; Hert, D. G.; Brennecke, J. F. Thermophysical properties of imidazoliun based ionic liquids. *J. Chem. Eng. Data* **2004**, *49*, 954–964.

(31) Jacquemin, J.; Ge, R.; Nancarrow, P.; Ronney, D. W.; Costa Gomes, M. F.; Pádua, A. A. H.; Hardacre, C. Prediction of Ionic Liquid Properties. I. Volumetric Properties as a Function of Temperature at 0.1 MPa. *J. Chem. Eng. Data* **2008**, *53*, 716–726.

(32) Ge, R.; Hardacre, C.; Nancarrow, P.; Rooney, D. W. Thermal Conductivities of Ionic Liquids over the Temperature Range from 293 to 353 K. *J. Chem. Eng. Data* **2007**, *52*, 1819–1823.

(33) Gardas, R. L.; Freire, M. G.; Carvalho, P. J.; Marrucho, I. M.; Fonseca, I. M. A.; Ferreira, A. G. M.; Coutinho, J. A. P. High-Pressure Densities and Derived Thermodynamic Properties of Imidazolium-Based Ionic Liquids. *J. Chem. Eng. Data* **2007**, *52*, 80–88.

(34) Gardas, R. L.; Freire, M. G.; Carvalho, P. J.; Marrucho, I. M.; Fonseca, I. M. A.; Ferreira, A. G. M.; Coutinho, J. A. P. PρT Measurements of Imidazolium-Based Ionic Liquids. *J. Chem. Eng. Data* **2007**, *52*, 1881–1888.

(35) Ye, C.; Shreeve, J. M. Rapid and Accurate Estimation of Densities of Room-Temperature Ionic Liquids and Salts. *J. Phys. Chem. A* **2007**, *111*, 1456–1461.

(36) Jenkins, H. D. B.; Roobottom, H. K.; Passmore, J.; Glasser, L. Relationships among Ionic Lattice Energies, Molecular (Formula Unit) Volumes, and Thermochemical Radii. *Inorg. Chem.* **1999**, *38*, 3609–3620.

(37) NIST Chemistry Webbook. http://webbook.nist.gov/chemistry/ (accessed Nov 17, 2009).

(38) Joback, K. G. *A unified approach to physical property estimation using multivariant statistical techniques*. M.Sc. Thesis in Chemical Engineering, Massachusetts Institute of Technology, Cambridge, MA, 1984.

(39) Poling, B. E.; Prausnitz, J. M.; O'Connell, J. P. *The Properties of Gases and Liquids*, 5th ed.; McGraw-Hill: New York, 2001.

(40) Sirjoosingh, A.; Alavi, S.; Woo, T. K. Molecular Dynamics Simulations of Equilibrium and Transport Properties of Amino Acid-Based Room Temperature Ionic Liquids. *J. Phys. Chem. B* **2009**, *113*, 8103–8113.

Received for review August 4, 2009. Accepted December 9, 2009. The authors would like to thank the UK EPSRC under a portfolio partnership for financially supporting this work. R.G., A.H., and P.G. acknowledge the funding from PETRONAS.

JE900660X